Orbital eccentricity as a probe of thick disc formation scenarios

Laura V. Sales,[1]* Amina Helmi,[1] Mario G. Abadi,[2] Chris B. Brook,[3]
Facundo A. Gómez,[1] Rok Roškar,[4] Victor P. Debattista,[3] Elisa House,[3]
Matthias Steinmetz[5] and Álvaro Villalobos[1]

[1]*Kapteyn Astronomical Institute, PO Box 800, Groningen, the Netherlands*
[2]*Universidad Nacional de Córdoba, Laprida 854, 5000 Córdoba, Argentina and Instituto de Astronomía Teórica y Experimental, Conicet, Argentina*
[3]*Centre for Astrophysics, University of Central Lancashire, Preston PR1 2HE*
[4]*Department of Astronomy, University of Washington, Box 351580, Seattle, WA 98195, USA*
[5]*Astrophysikalisches Institut Potsdam, An der Sternwarte 16, Potsdam 14482, Germany*

ABSTRACT

We study the orbital properties of stars in four (published) simulations of thick discs formed by (i) accretion from disrupted satellites, (ii) heating of a pre-existing thin disc by a minor merger, (iii) radial migration and (iv) gas-rich mergers. We find that the distribution of orbital eccentricities is predicted to be different for each model: a prominent peak at low eccentricity is expected for the heating, migration and gas-rich merging scenarios, while the eccentricity distribution is broader and shifted towards higher values for the accretion model. These differences can be traced back to whether the bulk of the stars in each case is formed *in situ* or is *accreted*, and is robust to the peculiarities of each model. A simple test based on the eccentricity distribution of nearby thick-disc stars may thus help elucidate the dominant formation mechanism of the Galactic thick disc.

Key words: Galaxy: disc – Galaxies: kinematics and dynamics – galaxies: formation.

1 INTRODUCTION

Several mechanisms have been proposed to explain the formation of thick discs in galaxies (see Majewski 1993). However, it is still unclear by which of these mechanisms thick discs preferentially form. This is despite the fact that more than 25 years have passed since it was first detected in the Milky Way (Gilmore & Reid 1983), and that it has been established that this component appears to be ubiquitous in late-type systems (e.g. Yoachim & Dalcanton 2008, and references therein).

Amongst the scenarios proposed to explain the formation of the thick discs are the direct accretion of stars from disrupted satellites (e.g. Abadi et al. 2003b), the thickening of a pre-existing thin disc through a minor merger (e.g. Quinn, Hernquist & Fullagar 1993; Kazantzidis et al. 2008; Villalobos & Helmi 2008), the scattering or migration of stars by spiral arms (e.g. Roškar et al. 2008; Schönrich & Binney 2009a,b) and *in situ* triggered star formation during/after gas-rich mergers (e.g. Brook et al. 2005; Bournaud, Elmegreen & Elmegreen 2007).

Even though studies of external galaxies have been fundamental to establish the statistical properties of thick discs, it is likely that only for the Galactic thick disc we will be able to unravel its evolutionary path. For example, measurements of the phase-space coordinates for nearby thick-disc stars allow reconstruction of their orbits, which contain imprints of the dynamical history, while their chemical abundances encode information about their sites of origin. Time is ripe to delve into more detailed predictions for the above-mentioned scenarios, because these have reached a level of maturity and detail that they warrant and permit a nearly direct comparison to observations.

In this Letter, we investigate how the orbits of thick-disc stars can be used to distinguish between the various formation channels. In particular, we focus on the predicted eccentricity distributions. We expect our findings to be applied soon to samples of nearby thick-disc stars from SEGUE (Smith et al. 2009; Yanny et al. 2009) and RAVE (Steinmetz et al. 2006; Breddels et al., in preparation), and in the long term, to the *Gaia* data set which will provide much more accurate information for much larger samples of stars spanning a wide range of distances from the Sun. The orbital eccentricity test should help to elucidate the dominant mechanism by which the Galactic thick disc formed.

2 NUMERICAL EXPERIMENTS

We have gathered four existing numerical simulations of late-type galaxies that, having all developed a thick-disc component, clearly differ in the dominant formation mechanism. These are (i) accretion and disruption of satellites (Abadi et al. 2003b), (ii) disc heating by a minor merger (Villalobos & Helmi 2008), (iii) radial migration via resonant scattering (Roškar et al. 2008) and (iv) *in situ* formation during/after a gas-rich merger (Brook et al. 2004, 2005).

*E-mail: lsales@astro.rug.nl

Table 1. Relevant parameters for each of the simulations.

Scenario	$M_{\rm vir}$ $(10^{10}\,{\rm M_\odot})$	$M_{\rm bulge}$ $(10^{10}\,{\rm M_\odot})$	$M_{\rm disc}$ $(10^{10}\,{\rm M_\odot})$	z_0 (thin) (kpc)	z_0 (thick) (kpc)	$R_{\rm d}$ (kpc)	ϵ (kpc)	Reference
Accretion	87	6.7	2.8	0.5	2.3	4.1	0.50	Abadi et al. (2003a,b)
Heating	50	–	1.2	–	1.2	–	0.01	Villalobos & Helmi (2008)
Migration	100	0.9	3.1	0.3	0.9	3.5	0.05	Roškar et al. (2008)
Merger	71	2.1	3.4	0.3	1.0	2.9	0.40	Brook et al. (2004)
Milky Way	60–200	1.	7–10	0.3	0.9	3.5	–	Turon et al. (2008)

Note: Columns are set as: (1) model, (2) virial mass, (3) bulge/spheroid mass (4) disc mass (thin+thick), (5) thin-disc scaleheight (from a double power-law fit to the vertical mass profile), (6) thick-disc scaleheight, (7) radial scalelength of the thin disc, (8) softening lengths and (9) reference to the original articles. For comparison, estimated values for the Milky Way have also been included. For the cosmological simulations, the virial masses are defined as the mass enclosed within the radius where the local density falls below $\Delta = 100$ times the critical density of the universe. A Hubble constant $H_0 = 70\,{\rm Mpc^{-1}\,km\,s^{-1}}$ is assumed when necessary. Disc scaleheights have been determined by fitting double-exponential laws to the vertical stellar density profile in the cylindrical shell $2 < R/R_{\rm d} < 3$.

2.1 Thick disc formation models

Because each of the simulations mentioned above have already been introduced in the literature, here we will only review their main relevant features, referring the reader to the original papers for further details. Table 1 summarizes their key parameters.

2.1.1 Accretion scenario

Abadi et al. (2003b) showed that within the Λcold dark matter paradigm, the accretion of stars from disrupting satellites in approximately coplanar orbits may give rise to an old thick-disc component that comprises about one-third of the mass of the much younger thin disc.

In our sample, we include the galaxy presented in Abadi et al. (2003b), which formed in a cosmological N-body/smoothed particle hydrodynamics (SPH) simulation. This object, with a virial mass of the order of that of the Milky Way, was selected from a low-resolution simulation of a large volume of the Universe and later re-simulated with much higher resolution. In this high-resolution run, the mass per baryonic particle is $\sim 3 \times 10^6\,{\rm M_\odot}$. The final mass for the thick disc in this galaxy (derived via a dynamical decomposition) is $1.1 \times 10^{10}\,{\rm M_\odot}$.

2.1.2 Heating scenario

In this model, a thick disc is formed by the dynamical heating that is induced by a massive satellite merging with a primordial, rotationally supported thin disc. This scenario has been explored recently by, for example , Villalobos & Helmi (2008) and Kazantzidis et al. (2008) who have shown that 5:1 mergers with a wide range of orbital inclinations generate thick discs whose properties are in reasonable agreement with observations. In such a model, the bulk of stars that end up in the thick disc originate from the primordial disc rather than from the accreted satellite (Villalobos & Helmi 2008).

In our analysis, we include one of the numerical experiments presented in Villalobos & Helmi (2008). In these simulations, the mass ratio between the satellite and the host is 0.2 and its initial orbit is prograde and inclined by $30°$ with respect to the host disc. The mass per stellar particle in the simulation is $m_{\rm p} = 1.2 \times 10^5\,{\rm M_\odot}$, and the thick disc has a final mass of $1.2 \times 10^{10}\,{\rm M_\odot}$. It is important to clarify that only a small fraction of the thin disc component is present at the end of the simulation (~ 15–20 per cent of the mass of the original disc). This implies that for this remnant to be the thick disc of a late-type galaxy, a new thin disc should form later from the cooling of fresh gas. This will lead to structural changes in the thicker component, which are not considered here. Nevertheless, if

the growth of the new disc is adiabatic then many characteristics, and in particular the eccentricities, are not expected to be dramatically different (Villalobos 2009).

2.1.3 Radial migration scenario

Stars in the thin disc may be trapped on to resonant corotation with spiral arms and may migrate inwards and outwards along the spiral waves approximately conserving their angular momenta (and hence eccentricity) and without leading to significant heating in the disc (Sellwood & Binney 2002). However, since the vertical velocity dispersion of stellar discs correlates with their surface brightness (Kregel, van der Kruit & Freeman 2005), the *radial migration* of stars from the inner regions (kinematically hotter) will result in the formation of a thicker disc component.

Although this process has not been formally proposed as a thick disc formation scenario, numerical simulations suggest that a modest thick component may be built. Therefore, we include in our sample the simulation presented in Roškar et al. (2008) run with the goal of characterizing the migration that takes place in galactic discs. The simulation starts with a dark matter halo of $\sim 10^{12}\,{\rm M_\odot}$ where 10 per cent of this mass is in the form of a hot halo gas component. This gas is allowed to cool and form stars self-consistently, mimicking the quiescent growth of disc galaxies, over a period of 10 Gyr. The initial mass resolution is $10^5\,{\rm M_\odot}$ for the baryons, and stellar particles have on average masses of $3 \times 10^4\,{\rm M_\odot}$.
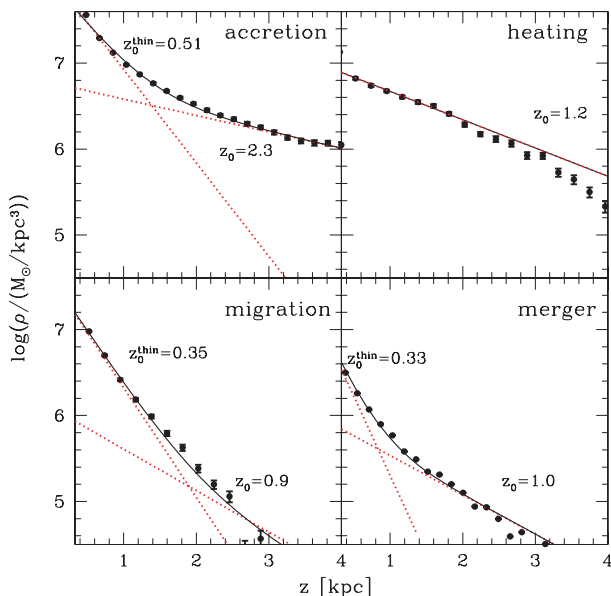
2.1.4 Gas-rich merger scenario

The last scenario we explore consists in the formation of a thick rotating component during an active epoch of gas-rich mergers in the past history of a galaxy (Brook et al. 2004, 2005). This formation channel differs fundamentally from the *accretion* model because the bulk of thick-disc stars is born *in situ* rather than being accreted from satellites. In this sense, this scenario might show certain similarities with the *heating* model. However, the latter requires the existence of a thin disc at early times, $z \gtrsim 1$, in contrast to the *merger* scenario where the stars are already born in a hotter component.

Here, we analyse the simulated galaxy introduced in Brook et al. (2004). It formed in a semi-cosmological N-body/SPH simulation that includes heating/cooling of gas, star formation, feedback and chemical enrichment. Its dark halo has a quiescent merger history after $z \sim 2$, and a final baryonic content of the galaxy is $\sim 5 \times 10^{10}\,{\rm M_\odot}$ (see Table 1). The mass per baryonic particle is $\sim 2 \times 10^5\,{\rm M_\odot}$. The mass of the thick disc in this galaxy is $\sim 2.2 \times 10^9\,{\rm M_\odot}$,

identified as old stars ($8.5 <$ age < 10.5) with relatively high rotation velocity ($V_{rot} > 50$ km s^{-1}).

The scenarios described in this section are capable of producing a rotationally supported hot component whose properties resemble the 'thick discs' in galaxies. However, the relative preponderance of such thick components does vary from galaxy to galaxy in our simulations. This is illustrated in Fig. 1, where we show with solid dots the vertical mass profiles for each case in a cylindrical shell $2 < R/R_d < 3$, which minimizes the contribution from bars and bulges. Additionally, in the accretion model, particles identified as 'spheroid' in Abadi et al. (2003b) have been removed (see Section 3). The error bars correspond to the rms obtained from 100 bootstrap re-samples of the data, and they are generally smaller than the dot sizes. The black solid lines show the best-fitting double exponential profile found for each galaxy, together with its decomposition into the 'thin' and the 'thick' disc contributions, in red dotted lines. This decomposition is generally robust, although correlations exist between the relative density of each component and the scaleheight of the thick disc. The scaleheights z_0 obtained by minimizing χ^2 are quoted in each panel, and the typical errors are of the order of $\sim$5–10 per cent for z_0^{thin} and $\sim$20–30 per cent for the thick component. For the migration scenario, the uncertainties are larger due to the stronger dominance of the thin disc and are 15 and 60 per cent for z_0^{thin} and z_0, respectively. Nevertheless, in all cases, the results presented below are robust to changes in the value of z_0 within the uncertainties.

Differences in the relevance of the thick component not only depend on the net efficiency of the respective formation process but may also be influenced by the different initial conditions and simulation techniques (e.g. only the *accretion* and *merger* scenarios actually account for the full cosmological framework). Because of these basic differences between simulations, global properties such as the mass, rotation and size of each formed thick disc are

expected to be diverse. Our focus, however, is on contrasting the specific dynamical properties of the stars in the thick component for each case, and in particular, their orbital eccentricities, which as we shall see below, are fundamentally related to the physical mechanism by which this component was built.

In order to facilitate comparisons between the thick discs in our galaxies and in particular also to that of the Milky Way, we rescale the radial and vertical distances of the stellar particles in each galaxy by their corresponding thin-disc scalelengths and thick-disc scaleheights.[1] In what follows, we will focus our attention on 'solar neighbourhood volumes', equivalent to cylindrical shells between two and three scaleradii of the thin disc ($2 < R/R_d < 3$). For comparison, $R_\odot/R_d \sim 2.2$–2.4, assuming a scale radius of $R_d = 3.5$ kpc for the Milky Way.

2.2 Modelling of the orbits

Kinematical surveys such as RAVE, SEGUE and ultimately *Gaia* provide phase-space coordinates of stars around the position of the Sun. This instantaneous information may be used to recover their plausible past orbits. This requires modelling the (unknown) Galactic potential, and possibly its evolution, which implies that the orbital parameters derived for each star generally suffer from a certain degree of uncertainty, even if measurement errors are neglected.

On the other hand, our numerical simulations allow us to track each particle in time, with full orbits that are known. Nevertheless, we prefer to mimic observations, and therefore we use the present-day position and velocity of each stellar particle as initial conditions for the integration of their orbits in the best-fitting potential of their host galaxy. We model each galaxy as a four-component system with an NFW (Navarro, Frenk & White 1997) dark halo, a Hernquist profile (Hernquist 1990) for the bulge and two Miyamoto–Nagai discs (Miyamoto & Nagai 1975) corresponding to the thin- and thick-disc contributions. The mass associated with each of these components is known for each simulation (see Table 1), and their various scalelengths are chosen by requiring a good match to the circular-velocity profile of the system up to a distance of 20 kpc[2]. This is along the lines of the previous work, where the circular velocity of the Milky Way is often used to constrain the model parameters (e.g. Helmi et al. 2006).

We define eccentricity as $\epsilon = (r_{ap} - r_{pe})/(r_{ap} + r_{pe})$, where r_{ap} and r_{pe} correspond, respectively, to the apocentre and pericentre distance of the last orbit of each particle. With this definition, for a circular-velocity curve modelled with $\sim$10 per cent accuracy, the eccentricities obtained by numerical integration show a scatter of $\pm$ 0.1–0.2 around their true value with no systematic trends (see Fig. 2). Larger deviations are found as the eccentricity increases.

3 RESULTS

Baryons in galaxies are generally sorted in several components: a bulge, a disc (thin + thick) and a more extended and diffuse spheroidal distribution, the stellar halo, that might extend well beyond the luminous edge of the disc. Although each of these

Figure 1. Vertical density profile of stars for each of the scenarios discussed in Section 2.1. The best-fitting mass-weighted double-exponential profiles are shown with black solid lines, and the individual contributions of the 'thin' and 'thick' components are indicated by the red dotted curves. Note that there is no significant thin disc in the *heating* scenario, thus only the vertical profile for the thick component is present. For the accretion scenario, kinematical cuts have been applied in order to avoid contamination from the stellar halo (see text for details).

[1] For the simulation by Villalobos & Helmi (2008), we assume the scalelength to be that of the Milky Way thin disc: $R_d = 3.5$ kpc, although our conclusions do not fundamentally depend on this choice.
[2] For the migration and merger scenarios only the *total* (thin + thick) mass of the disc is known. For these cases the relative mass ratio between the thin and thick components is also a free parameter.
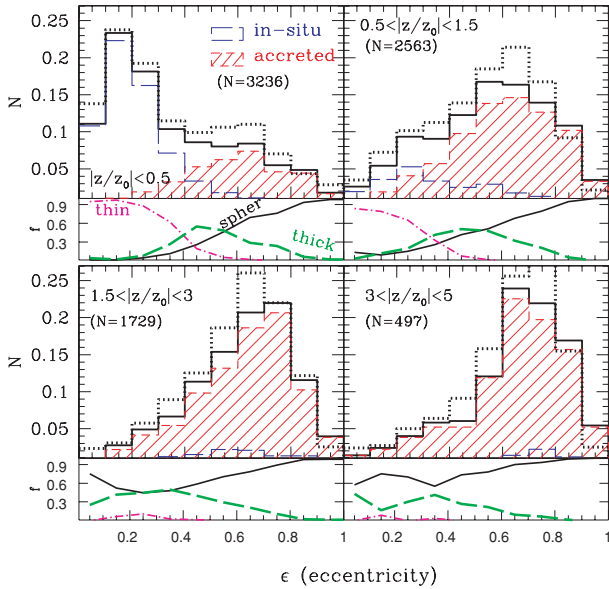
Figure 2. Eccentricity distribution of all stellar particles in a cylindrical shell with $2 < R/R_d < 3$ for the *accretion* scenario (Abadi et al. 2003b). The various panels are for different heights above/below the plane (normalized to the thick-disc scaleheight, z_0). The thick solid black line shows the total distributions per z bin, while blue-empty and red-shaded histograms distinguish between *in situ* and accreted stars. The effect introduced by the numerical integration of the orbits is rather small: the ϵ distribution obtained from direct tracking of the particle orbits in the simulation is shown in dotted black line. The fractional contributions from the thin disc (magenta dot–dashed), thick disc (green long-dashed) and the spheroid (solid black) to each eccentricity bin are shown below each histogram. The number of particles N included in each box is also quoted.

components has defining characteristics, some of its properties may change smoothly from component to component. For example, the eccentricity of the orbits changes as we move away from the disc plane into the realms of the stellar halo. This can be seen in Fig. 2, where the eccentricity distribution of all stellar particles within a cylindrical radii $2 < R/R_d < 3$ is plotted for different heights above/below the plane. Vertical distances are normalized to the scaleheight of the thick disc, z_0. The eccentricity distributions for stars formed *in situ* (defined as those born within a distance of 20 kpc from the main progenitor) and for those *accreted* are given by empty long-dashed blue and shaded red histograms, respectively. For comparison, the eccentricity distribution measured directly from the simulation (i.e. by tracking individual particle orbits) is given by the dotted histogram. This shows that no systematic errors are introduced by the orbital integration in the model host potential.

The lowermost bin $|z/z_0| < 0.5$ is largely dominated by thin disc stars with circular motions, as can be seen by the strong peak around $\epsilon \sim 0.15$ in the top-left panel of Fig. 2. These stellar particles formed *in situ* through local conversion of gas settled in a disc, into stars (blue empty histogram) within the main galaxy. As we move away from the plane, the thick disc gains importance and the eccentricity distributions become flatter as the fraction of accreted stars increases. Further above and below the plane, the distribution is dominated by particles from the spheroidal component, with even higher characteristic eccentricities, i.e. $\epsilon \sim 0.7$. These changes in the relative preponderance of the thin, thick and spheroidal components can be seen as their fractional contribution (magenta dot–dashed, green long-dashed and black solid, respectively) to each eccentricity on the bottom panel of all $|z|$ bins. Here, we have used the dynamical

decomposition performed in Abadi et al. (2003b) to assign stars to a given component.

This galaxy, introduced in Abadi et al. (2003a,b), has a large stellar spheroid that contains more than ~ 70 per cent of the total luminous mass. Fig. 2 shows that its contribution dominates the high-eccentricity bins at all heights above/below the plane. To highlight the properties of the thick disc, and also to avoid confusion on the interpretation of our results and its comparison with other simulated galaxies (lacking such a prominent spheroidal component), we will exclude in what follows any stellar particle that has been assigned to the spheroid by the analysis performed in Abadi et al. (2003b).

Fig. 3 shows how the eccentricity distributions vary according to the different formation channels of the thick disc. Each panel corresponds to one particular model: *accretion* (top-left panel), *heating* (top-right panel), *migration* (bottom-left panel) and *merger* (bottom-right panel). When relevant, the contributions from stars formed 'in situ' or 'accreted' have been highlighted. In order to minimize the contribution from thin disc stars, we have focused on the vertical bin $1 < |z/z_0| < 3$. On the other hand, to avoid contamination from the spheroids in our simulations (this is unlikely to be important for the Galactic stellar halo because of its very low density), we only consider stars with rotational velocity $v_\phi > 50$ km s^{-1}. This corresponds to average azimuthal velocity at which there is a clear excess of stars with velocities larger than this threshold compared with the distribution at $v_\phi < -50$ km s^{-1} in our simulations. Under the assumption of a non-rotating spheroidal component, this criterion will minimize the contribution of the stellar halo in our samples. None the less, we have checked that our results are not strongly sensitive to this assumption. The $v_\phi > 50$ km s^{-1} cut removes 33 per cent of the stars in Brook's model but has a negligible effect in the simulation by Villalobos & Helmi and Roškar et al. due to the suppressed contribution of satellite accretion. Recall that for the Abadi's galaxy, we have removed all the spheroid identified by the dynamical decomposition. Cuts on the cylindrical radii
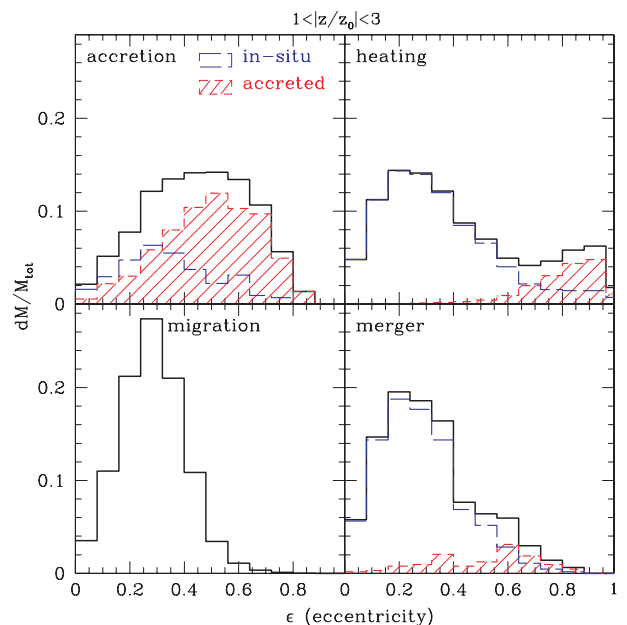
Figure 3. Comparison of the eccentricity distributions of each thick disc formation model for stars in the range 1–3 (thick disc) scaleheights and cylindrical distance $2 < R/R_d < 3$. The colour and line coding are the same as introduced in Fig. 2.

$(2 < R/R_d < 3)$ also help to elude the contributions from central bars and bulges.

Fig. 3 shows that the eccentricity distributions of stellar particles in these 'solar neighbourhood' regions, and between one and three thick-disc scaleheights above/below the plane, are different according to each model. For the *accretion* scenario, the distribution is very broad, with a median eccentricity $\langle \epsilon \rangle \sim 0.5$ (in good agreement with the accreted component in Read et al. 2008). On the other hand, the heating of a pre-existing thin disc by a minor merger gives rise to a bimodal distribution. The dominant peak is at low eccentricity $\epsilon \sim 0.2$–0.3 and associated with the stars from the progenitor disc, while the second peak at $\epsilon \sim 0.8$ is brought by the disrupted satellite. *Radial migration* tends to preserve the initial (low) eccentricity distribution, with only one peak present at $\langle \epsilon \rangle \sim 0.2$ and with a sharp cut-off at $\epsilon \sim 0.6$. Finally, in the *merger* scenario a prominent peak around $\epsilon \sim 0.2$ is visible which is associated with the stars formed *in situ* during the epoch of active gas-rich mergers. But as for the *accretion* scenario, accreted stars from infalling satellites contribute to a high-eccentricity tail.

Interestingly, Fig. 3 shows, as expected, that stars formed *in situ* have low-eccentricity orbits regardless of the mechanism (*heating, migration, merger*) that places them at their current height above/below the plane. On the other hand, accreted stars from satellites always dominate the high-eccentricity tails of the distributions. Changes in the relative proportion of *in situ* versus accreted stars drive the differences seen in the histograms of each thick disc formation scenario. In other words, the analysis of the stellar eccentricities off the plane helps to unravel whether the bulk of stars was formed locally in the main progenitor (*heating, migration, merger*) or, on the contrary, was accreted from infalling satellites (*accretion*).

Kolmogorov–Smirnov tests performed over randomly generated subsamples of stars selected from each simulation show that ~ 150 stars are enough to distinguish at 90 per cent confidence level between all the scenarios investigated here. Moreover, in samples containing more than ~ 550 stars, the probability that the stars are drawn from the same distribution is found to be lower than 1 per cent. Clearly, a smaller number of stars (~ 200) is sufficient to distinguish the accretion model from the rest. Note, however, that these estimates are only indicative since they are derived for particular realizations of a general class of models.

It is important to recall that each of these simulations has produced a galaxy with a different morphology. Furthermore, the simulations representative of the *heating* scenario as well as that of *migration* have, by construction, a suppressed contribution from accreted satellite galaxies. Nevertheless, the general behaviour of *in situ* versus *accreted* populations is robust to the different simulation idiosyncrasies and can be traced back to the different physical mechanisms related to where and how the stars were formed. Therefore, we do not expect the global properties of the eccentricity distribution (e.g. bimodality, high-eccentricity tails associated with accreted populations) to differ significantly, but only in the details, in other realizations of the same models. Although we have focused on 'solar-neighbourhood' regions $(2 < R/R_d < 3)$, our conclusions do not depend fundamentally on this choice.

4 CONCLUSIONS

In this Letter, we have analysed four numerical simulations of galaxies hosting a thick-disc component of fundamentally different origin: (i) accretion of satellites, (ii) heating of a pre-existing disc by a 5:1 mass-ratio merger, (iii) radial migration by resonant scattering and (iv) gas-rich mergers at high redshift.

We have compared the eccentricity distributions predicted by these different models for stellar particles in the 'solar neighbourhood', i.e. located in a cylindrical shell of radius $2 < R/R_d < 3$ and with heights $1 < |z/z_0| < 3$. Thick-disc stars formed *in situ* have low orbital eccentricities $\epsilon \sim 0.2$–0.3, independent of the mechanism that brought them high above/below the plane: gas-rich mergers, heating or migration. On the other hand, and again regardless of the particular model, accreted stars always dominate the high-eccentricity tail of the distributions. Therefore, the characterization of the eccentricity distribution of the thick disc can be used to establish if this component was formed by the accretion of satellites (Abadi et al. 2003) or alternatively locally within the main galaxy (Brook et al. 2005; Roškar et al. 2008; Villalobos & Helmi 2008). However, given the various limitations of our set of simulations, we cannot claim that it will be possible to make an unequivocal classification among models (i)–(iv) based only on eccentricity.

Nevertheless, the differences between the orbital eccentricities of *in situ* and accreted stellar particles are encouraging in view of the various kinematic surveys mapping our Galaxy today and in the near future. We believe that with a reasonable guess of the Milky Way potential, the analysis of the eccentricity distribution of thick-disc stars at approximately 1–3 scaleheights should shed light on the formation path of the Galactic thick disc.

REFERENCES

Abadi M. G., Navarro J. F., Steinmetz M., Eke V. R., 2003a, ApJ, 591, 499
Abadi M. G., Navarro J. F., Steinmetz M., Eke V. R., 2003b, ApJ, 597, 21
Bournaud F., Elmegreen B. G., Elmegreen D. M., 2007, ApJ, 670, 237
Brook C. B., Kawata D., Gibson B. K., Freeman K. C., 2004, ApJ, 612, 894
Brook C. B., Gibson B. K., Martel H., Kawata D., 2005, ApJ, 630, 298
Gilmore G., Reid N., 1983, MNRAS, 202, 1025
Helmi A. et al., 2006, MNRAS, 365, 1309
Hernquist L., 1990, ApJ, 356, 359
Kazantzidis S. et al., 2008, ApJ, 688, 254
Kregel M., van der Kruit P. C., Freeman K. C., 2005, MNRAS, 358, 503
Majewski S. R., 1993, ARA&A, 31, 575
Miyamoto M., Nagai R., 1975, PASJ, 27, 533
Navarro J. F., Frenk C. S., White S. D. M., 1997, ApJ, 490, 493
Quinn P. J., Hernquist L., Fullagar D. P., 1993, ApJ, 403, 74
Read J. I., Lake G., Agertz O., Debattista V. P., 2008, MNRAS, 389, 1041
Roškar R. et al., 2008, ApJ, 675, L65
Schönrich R., Binney J., 2009a, MNRAS, 396, 203
Schönrich R., Binney J., 2009b, MNRAS, in press (arXiv:0907.1899)
Sellwood J. A., Binney J. J., 2002, MNRAS, 336, 785
Smith M. C. et al., 2009, MNRAS, in press (arXiv:0904.1012)
Steinmetz M. et al., 2006, AJ, 132, 1645
Turon C. et al., 2008, The Messenger, 134, 46
Villalobos Á., 2009, PhD thesis, Univ. Groningen
Villalobos Á., Helmi A., 2008, MNRAS, 391, 1806
Yanny B. et al., 2009, AJ, 137, 4377
Yoachim P., Dalcanton J. J., 2008, ApJ, 682, 1004

This paper has been typeset from a TEX/LATEX file prepared by the author.